THE EFFECT OF FABRIC ARCHITECTURE ON THE PROCESSING AND PROPERTIES OF COMPOSITES MADE BY VACUUM ASSISTED RESIN TRANSFER MOLDING (VARTM)

Francois Ntakobatagize, Oscar Ntakontagize, Donald Klosterman

University of Dayton
Dayton, Ohio, USA

ABSTRACT

The goal of this research project was to evaluate and compare the effect of fabric architecture on the processing and properties of composites made by Vacuum Assisted Resin Transfer Molding (VARTM). The fabric architectures investigated included plain weave, satin weave, and warp-knit unidirectional. The fiber types included E-glass and standard modulus carbon fiber. Flat panels were fabricated with a lab scale VARTM process using an epoxy resin system. Fabric plies were cut to 45 cm x 30 cm (18 in. x 12 in.), and the number of plies used depended on the fiber areal weight of each fabric to produce panels of similar final thickness. The speed of resin infusion was recorded by visually monitoring the flow front which was visible through the bag. Fiber volume fraction was evaluated using thickness measurements, and porosity was investigated via optical microscopy. Mechanical testing was performed via tensile and 3-point flexure. The results showed the fabric type had minimal effect on the infusion speed with the exception of the plain weave and satin weave fiberglass. From the mechanical testing results, there are many comparisons made of the modulus, strength, and strain-to-failure results, for example carbon vs. glass, unidirectional vs. woven, tensile vs. flexure. The rule of mixtures was able to predict some but not all of these properties. The results, which are discussed in detail herein, illustrate the main advantage of selecting carbon vs. glass in stiffness driven applications.

1. INTRODUCTION

Fiber reinforced composite materials have many applications in different areas of society such as aerospace, marine, infrastructure, automotive, energy production, and sporting goods. When making new composite products, the designer is faced with an enormous number of material choices, including matrix composition, fiber composition, ply architecture (unidirectional, woven, knitted, braided, etc.), not to mention a large variety of fabrication processes. Fortunately there are several good handbooks available that compile information across the various types of materials and processes for polymer matrix composites [1-5].

There have been many studies reported in the literature over the past several decades that relate to VARTM processing [6-9]. Generally they can be classified in various ways, such as solid laminate vs. sandwich core composite, flat vs. curved geometry, room temperature vs. high temperature infusion, etc. In addition, there have been many good studies conducted to develop process models

SAMPE Conference Proceedings. Charlotte, NC, May 20-23, 2019. Society for the Advancement of Material and Process Engineering – North America.

and develop new materials for use in VARTM [10-13]. It is often difficult to make direct comparisons between the many published studies due to differences in processing parameters.

The project reported on herein was undertaken as a summer internship to provide undergraduate engineering students with a well-rounded immersion into composite material fabrication and testing. The primary technical goal of this project was to evaluate the effect of different fabric architectures on the processing and properties of flat composite laminates fabricated specifically through resin infusion. Three different fiber architectures were selected for each of fiberglass and carbon fiber materials, and flat panels were fabricated by Vacuum Assisted Resin Transfer Molding (VARTM). Process measurements included infusion speeds via visual monitoring. The quality of the panels was characterized through fiber volume fraction, microscopy, flexure testing, and tensile testing.

2. EXPERIMENTATION

2.1 Materials

The first step was to identify different fabric materials and characterize them to evaluate the effect of fabric architecture on molding results and resulting properties. Six different fabric materials available in our lab were identified for use, as summarized in Table 1. It was not possible to control every aspect of the experiment, for example the tow size and fiber composition of each fabric was not necessarily the same. However, the fiberglass materials were all E-glass type (modulus approximately 69-83 GPa, 10-12 MSI), and the carbon fabrics were standard modulus (227 GPa, 33 MSI) carbon fibers. Also, the processing parameters, operators, resin system, test methods and apparatuses were the same for all panels produced and tested.

First, the fiber areal weight (FAW) of each fabric was verified by cutting out and weighing a square of known area of each ply. Because there was a wide variation in FAW across all six fabrics, the number of fabric layers used for each panel was adjusted to yield the same total mass of fiber in each panel (about 370 g for fiberglass panels and 250 g for carbon panels). Photos of some of the fabrics are shown in Figure 1.

The resin system used in this study was EPON 862 (diglycidyl ether of Bisphenol F) and Epikure 3274 (comprised of about 80% polyoxypropylene diamine), both received from Resolution Performance Products LLC. They were mixed in stoichiometric proportions of 69 wt% EPON 862 and 31 wt% Epikure 3274. This resin system is commonly used for VARTM because of its low viscosity (approximately 0.1 Pa-sec) and ability to reach gelation at room temperature in about 6 hours. The cured resin modulus was approximated as 3 GPa for rule of mixture calculations.

Table 1. Fabric characteristics

Fiber Composition	Weave style	Designation in this study	FAW (g/m^2) (for one layer)	# layers in panel[1]	Total fiber weight (g) [1]
Fiberglass (E-glass)	Plain weave[2]	"Glass PW"	327	8	365
	8HS[3]	"Glass 8HS"	295	9	370
	Warp knit uni[4]	"Glass Uni"	440	6	368
Carbon (Std. Modulus)	Crowfoot (4HS)	"Carbon Crowfoot"	193	9	242
	5HS[5]	"Carbon 5HS"	370	5	258
	Warp knit uni[6]	"Carbon Uni"	227	8	253

[1] for panel of dimensions 45 cm x 30 cm (18 in. x 12 in.)
[2] style 7500, BGF Industries
[3] style 7781, Fibre Glast Developments Corp.
[4] Uni hotmelt yarn, Fiberglass Supply C72-5208
[5] 5HS BGF Industries 94900, 6k tow, modulus 227 GPa (33 MSI)
[6] Uni hotmelt yarn, Fiberglass Supply GAO60 C72-4825

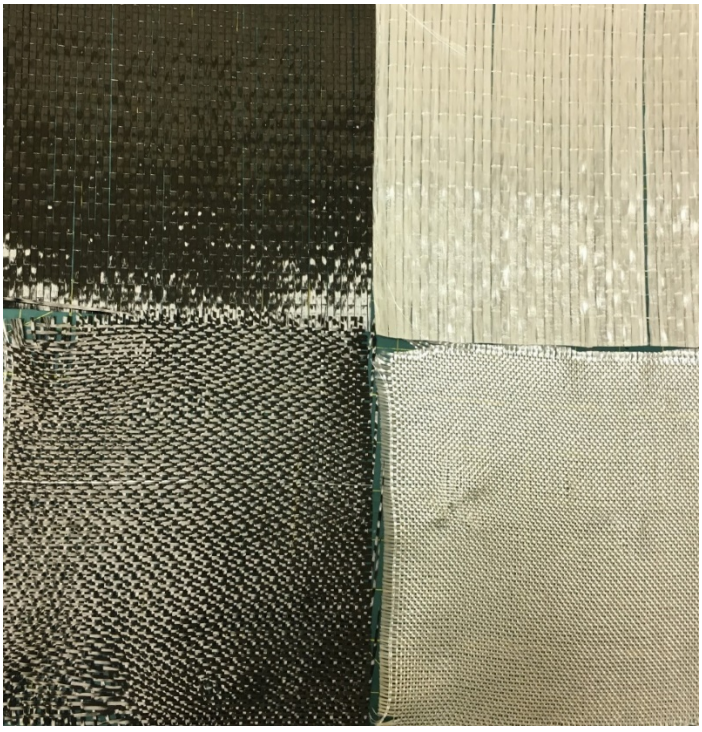

Figure 1: close up photograph of some of the fabrics, showing differences in fabric architecture - Carbon Uni (upper left), Glass Uni (upper right), Carbon 5HS (lower left), Glass 8HS (lower right).

2.2 Processing

All fabric layers for a given panel were cut to 45 cm x 30 cm (18 in. x 12 in.) dimensions, stacked on a metal VARTM table with the warp direction aligned in the same direction. Vacuum bag sealants was applied around the perimeter of the table, and a 5-cm-wide breather strip was placed just inside that (Figure 2A). Then a peel-ply was placed over the table including the perimeter breather strip, ending at vacuum bag sealant (Figure 2B). Next the resin infusion mat, vacuum bag, and resin feed port were installed (Figure 2C). The feed port was connected to a feed cup through a PVC tube (Figure 2D). Full details of the VARTM set-up can be found in a recent publication [14]. The infusion typically lasted 30 minutes or until the flow front was observed to reach the edge of the panel. During this time, the location of the flow front was marked on the bag with a black ink marker at 1-5 minute intervals. After the infusion was complete, the distance of the flow front at various times was measured and used to calculate resin flow front velocity. Each panel was left on the table under vacuum overnight. The next day it was removed from the table and post-cured in an oven at 100°C for 1 hour.

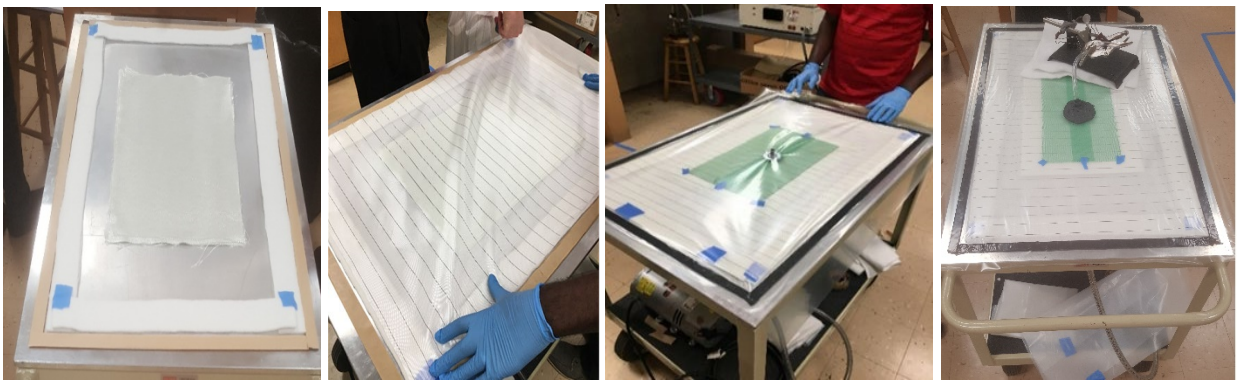

A **B** **C** **D**

Figure 2: Assembled vacuum bag and feed system.

2.3 Characterization

A wet saw with diamond blade was used to cut the panels into the various coupons needed for testing, as well as to remove the section immediately below the feed port (which was then discarded). Also, at least 1 small sample was cut out and potted in epoxy resin, polished with a Buehler AutoMet 250, and examined with an optical microscope to view the cross section for porosity and fiber uniformity. The uniformity of each panel's thickness was evaluated by using a digital calipers to measure the thickness of the tensile coupons (3 each) and flexure coupons (3 each). These six values were averaged and divided by the number of layers to calculate the average cured-ply-thickness (CPT). The average fiber volume fraction (V_f) was then calculated with Equation 1. The fiber density (ρ_f) was taken to be 2.54 g/cm^3 for fiberglass and 1.79 g/cm^3 for carbon. Note that Equation 1 relies on the assumption that there are no voids in the laminate.

$$V_f = FAW / (\rho_f \, x \, CPT) \tag{1}$$

Tensile testing was conducted via ASTM D3039. The tensile coupons were 25.4 cm long x 2.54 cm wide (10 in. x 1 in.), except for the panels containing unidirectional fibers which were 25.4 cm long x 1.27 cm wide (10 in. x 0.5 in). Each tensile coupon was further modified by adding 5-cm wide (~2 in.) fiberglass tabs to each end, as well as a bonded strain gage to the middle of the coupon on one side. Three coupons from each panel were tested. The testing was conducted with an Instron model 5985 materials testing system, using wedge action grips and extension rate of 2.54 mm/min (0.1 in/min). Flexure testing was conducted via ASTM D790 with a span-to-depth ratio of 32:1 and crosshead speed of 5.08 mm/min (0.2 in/min). Crosshead motion was used to provide displacement measurements. In previous work with similar materials, a deflectometer was used to verify that the crosshead motion provided an accurate measurement of deflection at the bottom center of the coupon. The flexure coupons were 1.27 cm wide (0.5 in.), and three coupons from each panel were tested. For both tensile and flexure testing, the modulus was calculated from the data between strain values of 0.1-0.3%.

3. RESULTS

3.1 Panel Fabrication

Photographs of a panel during and after infusion are given in Figure 3. The feed tube left an approximately 5-cm diameter flaw in the center of the panel. Therefore, mechanical testing coupons were cut out from other sections of the panel. All panels were fully infused, with no dry spots observed on the bottom.

A **B** **C**

Figure 3: A) Visual monitoring of infusion rate, B) end of infusion (feed tube clamped, bag under pressure overnight, and C) three fiberglass panels after unbagging and post cure.

An example of the resin flow front results is given in Figure 4. The resin flowed quickly through the highly porous green infusion mat at a nearly linear rate. Next the resin slowed down as it flowed over the bare fabric due to its lower permeability, and it was observed to proceed also at a linear rate. After penetrating to the perimeter of the panel, the resin then could only flow through the peel ply toward the vacuum perimeter. This rate was observed to be similar to the flow through the fabric.

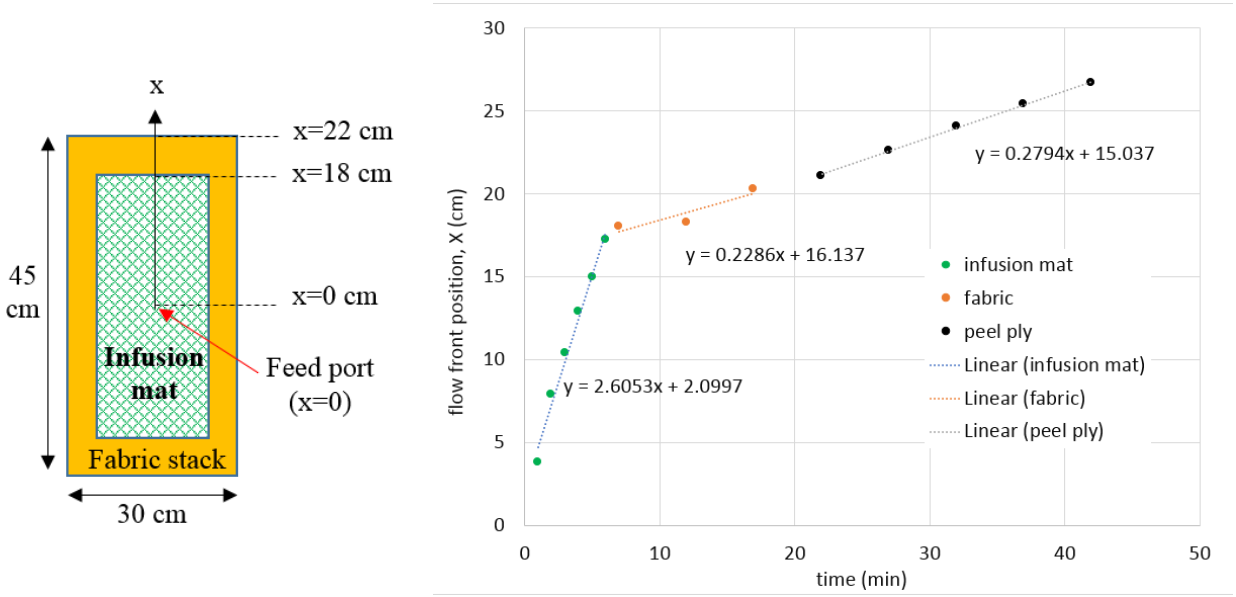

Figure 4: (left) diagram of VARTM set-up and dimensions, and (right) example flow front result.

The full results are summarized in Table 2. The most noticeable result is how much faster the resin flowed through the infusion mat than over the bare fabric. This demonstrates the purpose of an infusion mat: it quickly distributes the resin over a large area and allows the resin time to seep down through the panel before it reaches the edge of the panel. The mat usually does not extend to the very edge of the panel: the purpose of this is to prevent resin that might reach one side sooner than the other from "race-tracking" around the perimeter and cutting off dry spots. In our set-up, we maintained a 5-cm gap between the edge of the mat and edge of the panel. The edge of the panel was at least 15 cm from the nearest vacuum perimeter. This gap was covered only by the peel ply (and vacuum bag). Thus, there were several "brakes" set in place to prevent the resin from reaching the vacuum source before the panel had time to fully infuse.

The flow front velocity through the infusion mat was approximately 1.2 cm/min, except for the first two panels fabricated (glass plain weave at 3.69 cm/min, and 8HS at 3.46 cm/min). We are not certain whether this result was affected by the fabric type, or some unintended process difference like the vacuum level (less vacuum would cause a loose bag and faster flow) or perhaps the feed tube details. The fabric permeability could affect the flow velocity in the distribution mat above it because the flow through these two materials is coupled. A low permeability fabric (high resistance to flow) would force more flow through the distribution mat (higher velocity). A high permeability mat (low resistance) would allow an alternate path for flow and therefore slow down the flow through the mat above. The plain weave and 8HS glass fabrics were expected to be the *highest* permeability fabrics (low resistance to flow), so these would be expected to have the *lowest* velocity in the infusion mat (counter to observed results). In any case, this topic is of interest for future study. Measuring the permeability of the fabrics and/or performing a fluid mechanics analysis of the flow were beyond the scope of this project.

Table 2: flow front velocity results

Fabric Type	Flow front velocity (cm/min)	
	Infusion mat	fabric
Glass PW	3.69	0.09
Glass 8HS	3.46	0.08
Glass Uni	1.29	0.08
Carbon Crowfoot	1.03	0.09
Carbon 5HS	1.35	0.09
Carbon Uni	1.23	0.10

3.2 Physical Properties & Microscopy

Thickness and fiber volume fraction (V_f) results are summarized in Table 3 and Figure 5. The V_f of the fiberglass panels was between 0.4-0.5, which is typical for fiberglass / VARTM. The plain weave fiberglass panel had the lowest V_f of the glass panels, and the unidirectional panel had the highest. This trend was expected due to layer packing efficiency: the plain weave architecture (each tow goes over 1 / under 1 tow) is very "bumpy" and include a lot of open space, while unidirectional lays flat and has less open space. Also, any possible vacuum bag issue, as raised by the flow front results, may have reduced V_f. The trend was similar with the carbon panels, with the "flattest" fabric (unidirectional) having the highest V_f, and the most "bumpy" (crowfoot) having the lowest V_f. However, V_f of the carbon panels were all very close. Overall the carbon panels had significantly higher V_f than fiberglass due to the small size of carbon fibers and ability to pack efficiently. The V_f results for carbon were considered to be pretty good for the simple VARTM process used. To obtain higher values often required in aerospace, such as 0.60-0.65, an autoclave or press could be used.

Table 3: Thickness and fiber volume fraction results for cured panels.

Fabric Type	Panel Thickness[1] (mm) / COV[2]	CPT (mm)	V_f
Glass PW	2.476 / 0.6%	0.310	0.416
Glass 8HS	2.430 / 5.9%	0.270	0.430
Glass Uni	2.177 / 4.8%	0.363	0.478
Carbon Crowfoot	1.780 / 2.2%	0.198	0.545
Carbon 5HS	1.810 / 0.9%	0.362	0.571
Carbon Uni	1.755 / 2.2%	0.219	0.578

[1] this value is the average of three tensile coupons and three flexure coupons
[2] Coefficient of Variation (COV) = standard deviation / mean

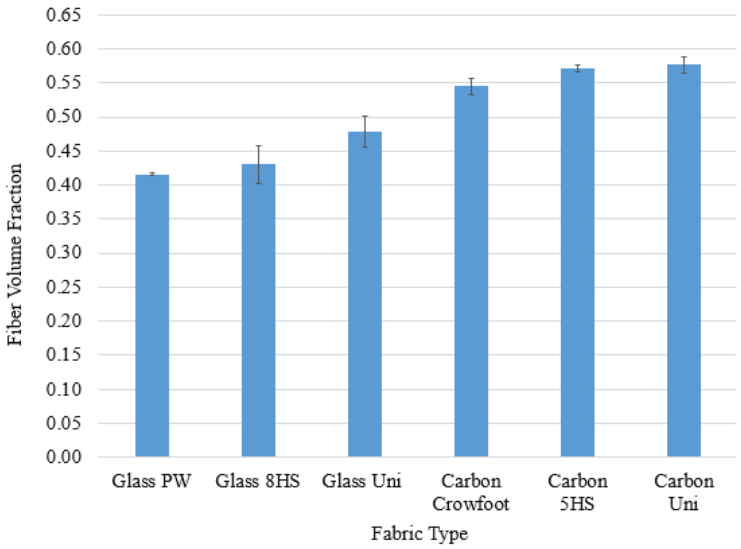

Figure 5: V_f results calculated from thickness values of the six mechanical test coupons (3 tensile, 3 flexure). The error bars represent ±1 standard deviation.

Example photomicrographs of some panels are given in Figure 6. In general, there was little or no porosity in all panels. However, there were resin rich areas in the fabric panels where tows cross each other and in between plies, which helps explain the V_f results.

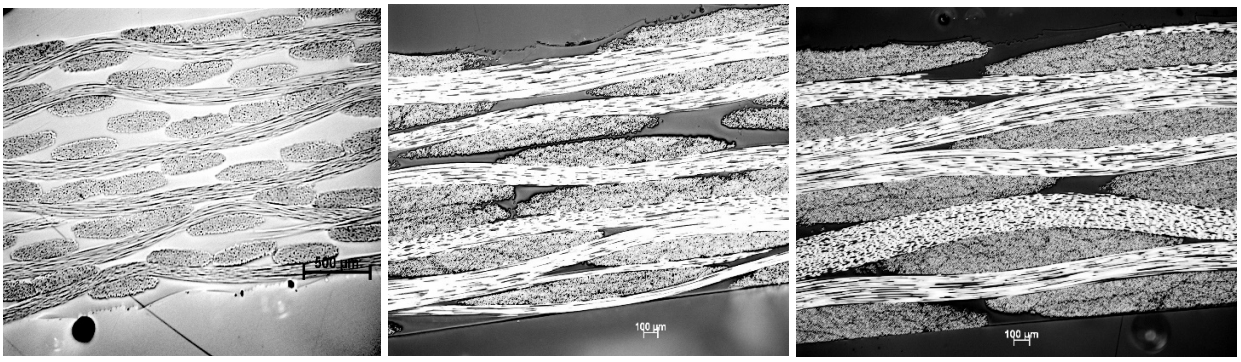

A **B** **C**

Figure 6: Photomicrographs of polished cross section at 50X magnification: A) Glass 8HS, B) Carbon Crowfoot, and C) Carbon 5HS. The open spaces between tows is filled with resin.

3.3 Mechanical Properties

The tensile coupons generally failed in the gage section, although some failed simultaneously in the gage and near the tab. The flexure coupons failed by axial compression on the top face. The stress-strain curves were linear up to at least 1% strain with both tests (see Figure 7). Any non-linearity occurred near the failure point. Only the unidirectional glass flexure coupons exhibited significant stair-stepping after the initial load-drop. Although not shown here, one of each of the carbon tensile coupons exhibited a "wiggly" stress-strain curve, which was traced to noise in the strain gage response (load smoothly increased). We did not resolve if this was a mechanical effect

(foil strain gage bonding problems) or an electronic signal issue. None of the fiberglass tensile coupons had this problem.

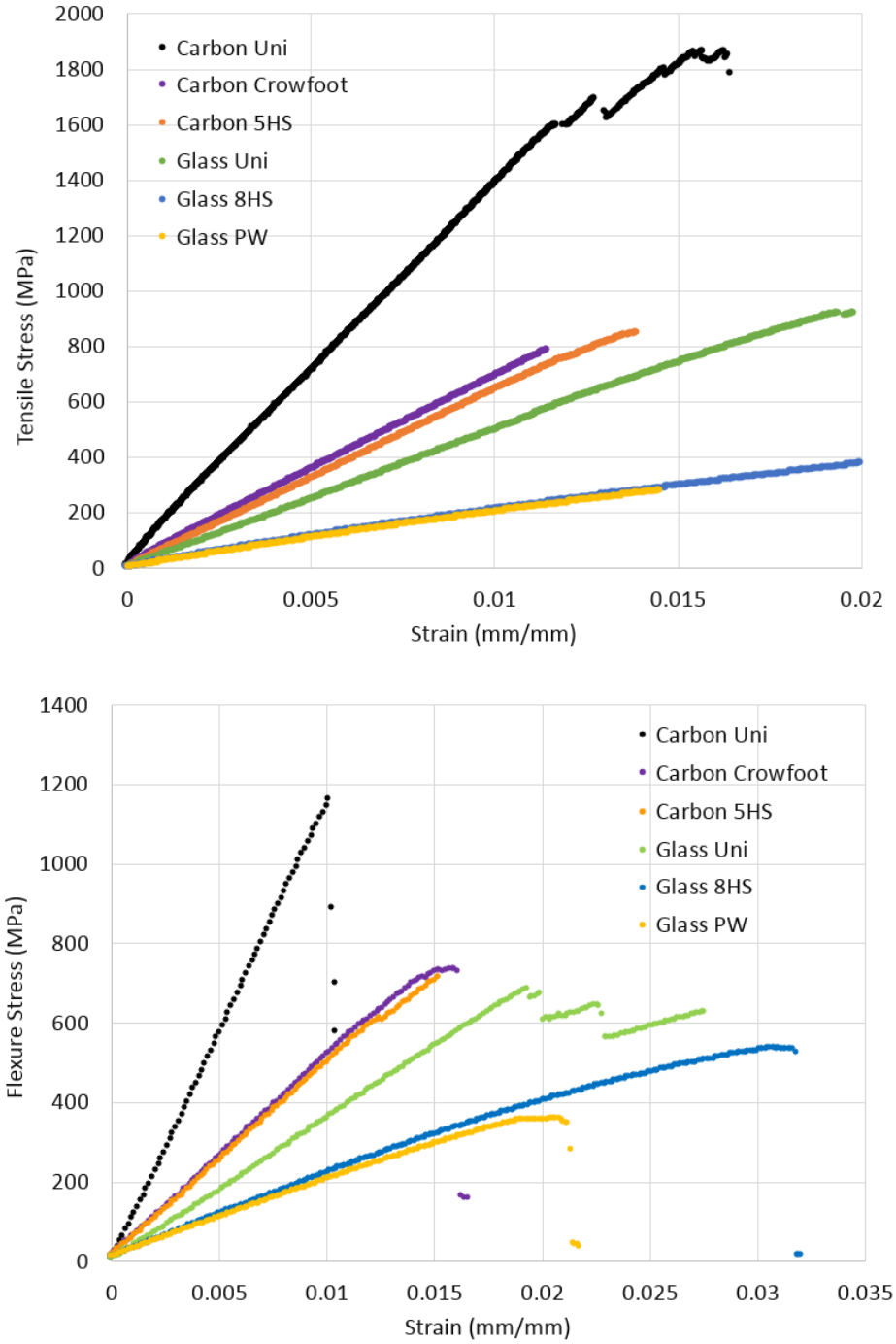

Figure 7: example stress-strain curves for tensile coupons (top) and flexure coupons (bottom). These curves have NOT been normalized for fiber volume fraction, but they are shown here to demonstrate overall shape and relative linearity.

The effective fiber volume fraction of each coupon was calculated with Equation 1 using its measured thickness. This V_f value was used to normalize the modulus and strength value of each coupon to an equivalent coupon with 50% fiber volume fraction (for example, $E_{Vf,50\%} = E_{measured} \times 0.5 / V_{f,measured}$). This normalization is commonly done to make better comparisons between composite material systems with different degrees of compaction. For tensile coupons, this practice actually removes the uncertainty in the measured thickness because this value cancels out in the calculation (i.e. thickness is a linear factor in the denominator of $E_{measured}$ and $V_{f,measured}$). The tensile and flexure results are shown graphically in Figures 8-10 and in tabular form in the Appendix.

The modulus results are given in Figure 8. First the tensile results will be discussed. Perhaps the best result to initially focus on is the tensile modulus of the unidirectional panels. These should be the "best behaved" property since the fibers are oriented in only one direction, and modulus is not very sensitive to defects such as porosity or non-uniform resin distribution. The tensile modulus of the carbon panel was close to that predicted by Rule of Mixtures "ROM" (122±7 GPa measured, compared to 227 GPa x 0.5 + 3 GPa x 0.5 = 115 Pa predicted by ROM). However, the modulus of the unidirectional glass panel was significantly *higher* than expected (50 GPa measured, compared to approximately 75 GPa x 0.5 + 3 GPa x 0.5 = 39 GPa predicted by ROM). This trend was also seen for the fabric panels, with the carbon fabric panels having only 2X higher modulus than glass fabric panels rather than 3X. On the other hand, the modulus values of the glass fabric panels in this study (26 GPa) are near those given in established handbooks, such as [2] which documents values of 22.7-25.6 GPa normalized for V_f =50% for three different glass / epoxy panels using 8HS and plain weave fabrics. Also, lamination theory calculations (not included here) indicate that the crossply laminate modulus should be approximately 24 GPa.

One result that was successfully predicted by ROM was that the tensile modulus of the unidirectional panels was about twice that of the fabric panels, since there were twice the number of fibers oriented in the test direction. There was not a significant difference when comparing the tensile modulus of the two woven carbon panels, as well as the two woven glass panels (i.e. weave style had no significant effect on tensile modulus).

Next, the flexure modulus results are discussed (Figure 8, orange bars), where the trends were similar to the tensile results. The flexure modulus of the carbon panels were only about 2X higher than the corresponding fiberglass panels. The modulus of the unidirectional carbon panel was about 2X higher than the fabric panels as expected, but the unidirectional glass panel was a little lower than expected compared to the fabric panels. The weave style did not significantly affect the flexure modulus results for either glass or carbon.

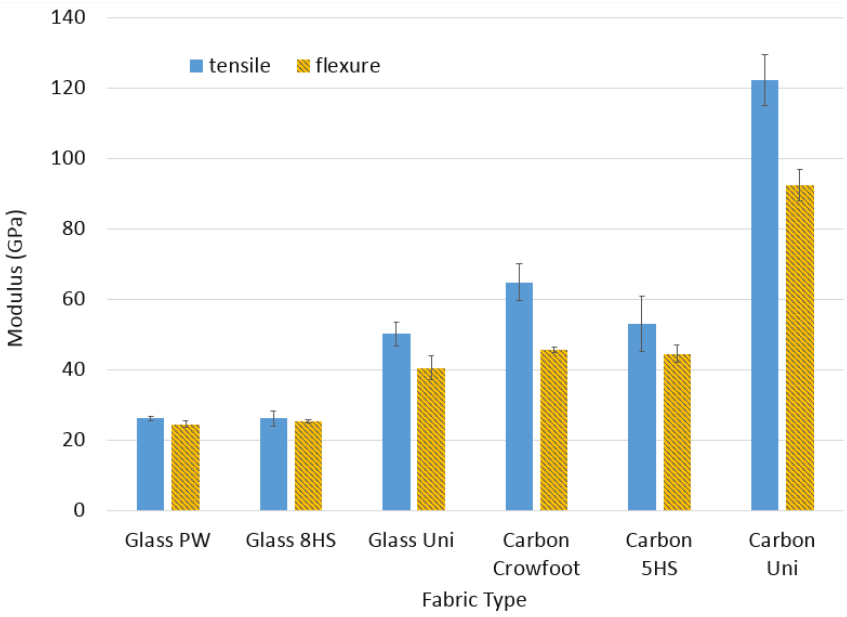

Figure 8: modulus results (normalized for V_f=0.50). The error bars represent ±1 standard deviation.

The strength results are given in Figure 9. The *tensile* strength of the unidirectional panels was a little more than 2X the corresponding fabric panels. However, the *flexure* strength of the unidirectional panels was only about 25% higher than the woven panels. This result was attributed to the nature of the flexure failure mechanism, which was axial compressive in the upper face sheet. This failure is expected to be sensitive to fabric architecture / flatness, as well as defects. When comparing carbon to glass, only the *tensile* strength of the *unidirectional* panels exhibited a large difference (about 2X comparing carbon uni to glass uni). In all the other comparisons (uni vs. woven, tensile vs. flexure, carbon vs. glass,), there were only small differences in strength. The average strength value across all panels (excluding uni carbon) and for both test methods was about 650 MPa. For comparison, results given in established handbooks [2] indicate a tensile strength of 330-520 MPa for woven glass and about 530 MPa for woven carbon laminates at 50% V_f. These results imply that selecting carbon vs. glass for a given application would be driven by modulus/stiffness requirements rather than ultimate strength.

The strain to failure results are given in Figure 10. The glass fiber laminates generally exhibited about 1.5X higher strain to failure than carbon. We expected the carbon strain-to-failure to be more near 2%, but there are some references in the literature for carbon fabric composites that report around 1% [2]. The unidirectional tensile coupons (carbon and glass) failed suddenly and explosively in the gage section. This is typical for tensile testing of unidirectional laminates and indicates the tabs and grips were working properly. On interesting trend was that the strain to failure of *unidirectional* panels was higher than fabric panels in *tensile* testing but the opposite in *flexure*. This was attributed to the quick build-up of compressive stress in the top face of the unidirectional flexure specimens and eventual failure in compression (where fibers are weaker in compression than in tension).

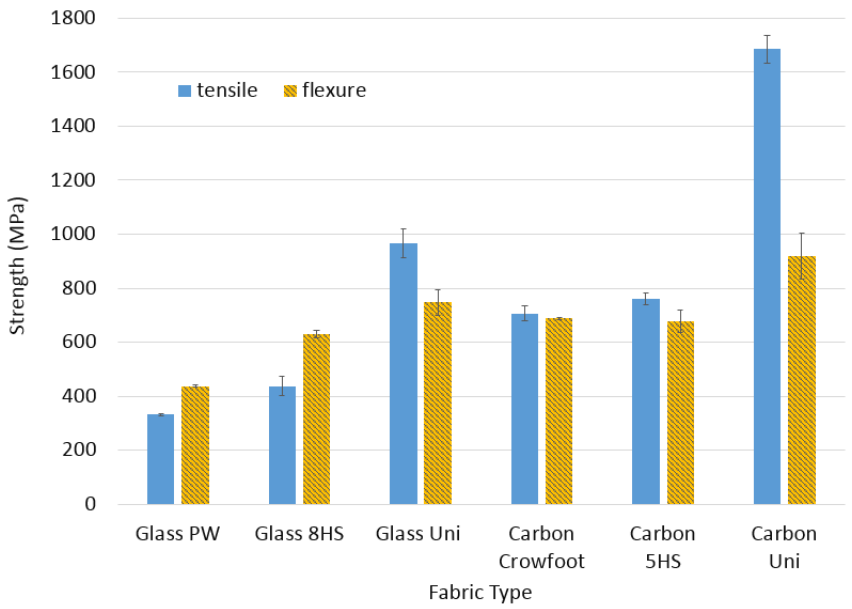

Figure 9: strength results (normalized for V_f=0.50). The error bars represent ±1 standard deviation.

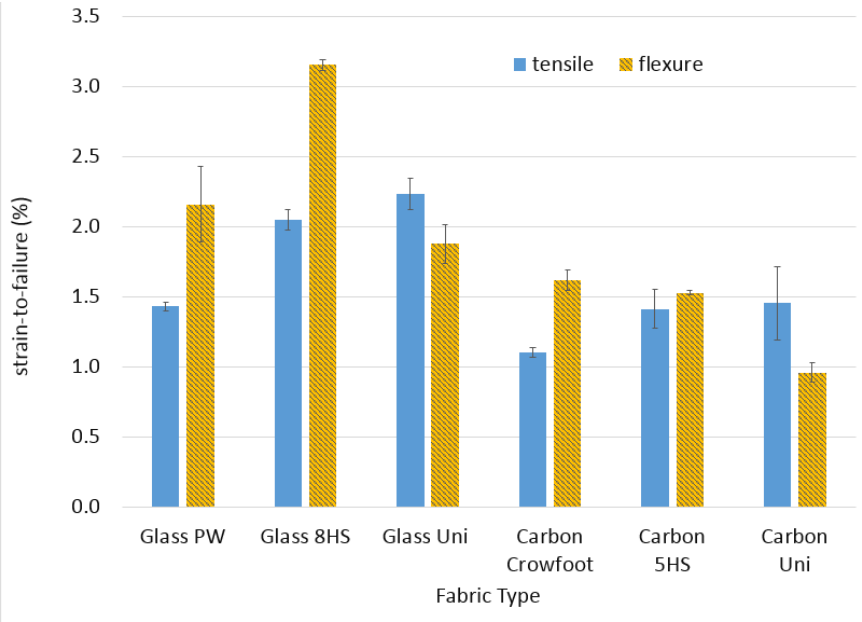

Figure 10: strain-to-failure results. The error bars represent ±1 standard deviation.

4. SUMMARY & CONCLUSIONS

This study constituted a fairly well controlled experiment to compare the processing and properties of six different fabric materials. Three fiberglass and three carbon panels of various fabric architectures were successfully molded using a vacuum resin infusion process. The fabric architecture had no significant effect on the infusion speed, except for the woven fiberglass panels. The fiber volume fraction of those two panels was lower than expected, possibly indicating there was a problem with the vacuum level or bagging material for those runs. This warrants further study to determine if the result is repeatable or a processing artifact. Microscopy results indicated that all the panels were well infused with little or no porosity. The fiber volume results were in a typical range for VARTM: 40-50% for glass and 50-60% for carbon. The unidirectional panels had higher volume fraction than the woven panels as expected due to more efficient packing of fibers.

The modulus results were in the range of that published in handbooks for comparable commercial systems, except the unidirectional glass tensile modulus which was about 25% higher than expected. The rule of mixtures was able to predict some of the modulus results successfully but not others. For example, based on the modulus values of the fibers, one would expect the carbon panels to be *three* times stiffer than the E-glass panels in tension and flexure. However, the results measured in this study, which are consistent with other published results, is that the modulus of the carbon panels is only about *two* times as high as the E-glass panels.

The strength of the panels were in the typical range for carbon and glass for both tensile and flexure. One interesting result was related to the comparison of unidirectional vs. woven panels. For *tensile* testing, the strength of uni panels was about twice that of fabric panels as expected by rule of mixtures. However, for flexure testing the unidirectional panels were only about 25% stronger. Furthermore, the strain-to-failure results for unidirectional panels was *higher* than fabric panels in tension testing but *lower* in flexure testing. These results were attributed to the failure mode in flexure which was compressive failure in the top face.

Overall this study provided a nice body of experimental data for highlighting differences in mechanical properties and fiber volume fraction in VARTM-molded carbon and glass laminates. The results illustrate the main advantage of selecting carbon over glass: the laminate modulus will be approximately twice, as well as have a lower density. The strength value is also improved, although not as dramatically as modulus. Thus, for applications requiring high specific strength and stiffness, the choice of carbon over glass is clearly illustrated.

5. ACKNOWLEDGMENTS

The authors wish to thank the Summer Undergraduate Research Experience (SURE) at the University of Dayton (U.D.) for providing student funding. Also, all materials, supplies, and access to equipment was provided by the Chemical & Materials Engineering Department at U.D.

6. REFERENCES

1. Composite Materials Handbook-17 (CMH-17), Volume 1: Polymer Matrix Composites - Guidelines for Characterization of Structural Material, SAE International, 2012.
2. Composite Materials Handbook-17 (CMH-17), Volume 2: Polymer Matrix Composites - Materials Properties, SAE International, 2012.
3. Composite Materials Handbook-17 (CMH-17), Volume 3: Polymer Matrix Composites - Materials Usage Design and Analysis, SAE International, 2012.
4. *ASM Handbook, Volume 21 Composites,* ed. D.B. Miracle, S.L. Donaldson, ASM International, Materials Park, Ohio, 2001
5. *Handbook of Composites*, ed. G. Lubin, Van Nostrand Reinhold Company Inc., New York, 1982.
6. Brouwer, W.D., van Herpt, E.C.F.C., Labordus, M. "Vacuum injection molding for large structural applications." *Composites: Part A* 34 (2003): 551-558.
7. Stoll, F., Klosterman, D., et al. "Design, Fabrication, Testing, and Installation of a Low-Profile Composite Bridge Deck." *SAMPE 2002 Conference Proceedings*, Long Beach, California, May 13-17, 2002, CD-ROM.
8. Yamashita, M., Sakagawa, T., Takeda, F., Kimata, F., Komori, Y. "Development of Advanced Vacuum-assisted Resin Transfer Molding Technology for Use in an MRJ Empennage Box Structure, *Mitsubishi Heavy Industries, Ltd., Technical Review* Vol. 45 No.4, Dec. 2008.
9. Bowman C.L, Roberts G.D, Braley M, Xie M & Booker M. "Mechanical Properties of Triaxial Braided Carbon/Epoxy Composites." *Proceedings of the 35th International SAMPE Technical Conference,* 2003, Dayton, OH. CD-ROM
10. Grimsle,y BW, Hubert, P., Xiaolan, S., Cano R.J., Loos, A.C., Pipes R.B. "Flow and compaction during the vacuum assisted resin transfer moulding process." *Proceedings of the 33rd International SAMPE Tech Conference*, 2001, 33:140–53. CD-ROM
11. Loos, A.C., Sayre, J., McGrane, R., Grimsley, B. "VARTM Process Model Development." *Proceedings of the 33rd International SAMPE Tech Conference*, 2001 CD-ROM.
12. Hammami, A. "Effect of Reinforcement Structure on Compaction Behavior in the Vacuum Infusion Process." *Polymer Composites*, June 2001, Vol. 22, No. 3.
13. Correiaa, N.C., Robitaillea, F., Longa, A.C., Rudda, C.D., Simacekb, P.,Advanib, S.G. "Analysis of the vacuum infusion moulding process: I. Analytical formulation." *Composites: Part A* 36 (2005) 1645–1656.
14. Klosterman, D.A., "Development of a Simple Lab-Scale Vacuum Assisted Resin Transfer Molding (VARTM) Process," *Proceedings of 2018 CAMX (Composites and Advanced Materials Expo)*, ACMA and SAMPE, Dallas, TX, October 2018.

APPENDIX

Tensile Results

Fabric Type	Modulus[1] / stdev[2] (GPa)	Strength[1] / stdev[2] (MPa)	Failure strain / stdev [2] (%)
Glass PW	26.1 / 0.6	332/ 4	1.43 / 0.03
Glass 8HS	26.1 / 2.1	437 / 36	2.05 / 0.07
Glass Uni	50.1 / 3.4	966 / 53	2.23 / 0.12
Carbon Crowfoot	64.8 / 5.2	707 / 26	1.10 / 0.03
Carbon 5HS	52.9 / 7.8	761/ 23	1.41 / 0.14
Carbon Uni	122.2 / 7.2	1686 / 51	1.46 / 0.26

3-Point Flexure Results

Fabric Type	Modulus[1] / stdev[2] (GPa)	Strength[1] / stdev[2] (MPa)	Failure strain / stdev [2] (%)
Glass PW	24.5 / 0.9	437 / 3.6	2.16 / 0.27
Glass 8HS	25.3 / 0.4	631 / 13.3	3.15 / 0.04
Glass Uni	40.5 / 3.4	748 / 47.3	1.88 / 0.14
Carbon Crowfoot	45.6 / 0.8	688 / 3.0	1.62 / 0.07
Carbon 5HS	44.5 / 2.4	677 / 41.2	1.53 / 0.01
Carbon Uni	92.4 / 4.6	918 / 86	0.96 / 0.07

[1] average result for three coupons. The result for each coupon was normalized for V_f=0.5 using its thickness to calculate V_f.
[2] standard deviation